



ELSEVIER

Nuclear Instruments and Methods in Physics Research A 464 (2001) 445–451

**NUCLEAR
INSTRUMENTS
& METHODS
IN PHYSICS
RESEARCH**
Section A

www.elsevier.nl/locate/nima

Induction accelerator efficiency at 5 Hz

A.W. Molvik^{a,*}, A. Faltens^{b,1}^aLawrence Livermore National Laboratory, University of California P.O. Box 808, L-645, Livermore, CA 94550, USA^bLBNL, MS 47-112, Berkeley, CA 94720, USA

Abstract

We simulate fusion power plant driver efficiency by pulsing small induction cores at 5 Hz (a typical projected power plant repetition rate), with a resistive load in the secondary winding that is scaled to simulate the beam loading for induction acceleration. Starting from a power plant driver design that is based on other constraints, we obtain the core mass and acceleration efficiency for several energy ranges of the driver accelerator and for three magnetic alloys. The resistor in the secondary is chosen to give the same acceleration efficiency, the ratio of beam energy gain to energy input to the core module (core plus acceleration gap), as was computed for the driver. The pulser consists of a capacitor switched by FETs, Field Effect Transistors, which are gated on for the desired pulse duration. The energy to the resistor is evaluated during the portion of the pulse that is adequately flat. We present data over a range of 0.6–5 μ s pulse lengths. With 1 μ s pulses, the acceleration efficiency at 5 Hz is measured to be 75%, 52%, and 32% for thin-tape-wound cores of nanocrystalline, amorphous, and 3% silicon steel materials respectively, including only core losses. The efficiency increases for shorter pulse durations. © 2001 Elsevier Science B.V. All rights reserved.

PACS: 52.58.Hm; 52.75.Di; 75.50.Kj; 75.50.Bb; 75.60.Ej

Keywords: Acceleration; Cores; Driver

1. Introduction

Induction accelerators hold the promise of accelerating large currents of ions (100s–1000s of amperes, in multiple beamlets) to GeV range energies with high efficiency [1]. In this paper, we experimentally model the efficiency of an induction linac that would accelerate Kr^+ ions to 1.3 GeV with a final beam energy of 3.3 MJ. Induction core

losses are taken to be the primary limitation on efficiency. Near the beginning of the accelerator, transport through quadrupoles limits the current in each beamlet. At the high-energy end the current is limited by the minimum beam duration of ~ 200 ns, which is set by core and pulser rise-time limitations at acceptable cost. These high currents are achieved by means of multiple (50–200) parallel beamlets, each of 0.5–1.0 A at the injector, and each increasing in current inversely with the beam duration as that is decreased during acceleration.

Throughout this paper, we choose some parameters that are technically challenging to accomplish, with a goal of subsequently determining

*Corresponding author. Tel.: +1-925-422-9817; fax +1-925-424-6401.

E-mail address: molvik1@llnl.gov (A.W. Molvik).

¹Participants in the Heavy Ion Fusion Virtual National Laboratory.

whether the cost advantages to a power plant are sufficiently compelling to justify the program necessary to develop the technical capability of achieving or surpassing the parameters. For example, the Kr^+ beams must be neutralized to $\sim 99\%$ to hit the appropriate spot size on the target, if the ions strip to charge states no higher than Kr^{4+} in the target chamber, with a conventional focusing system followed by a beam neutralizer.

We were conservative in three areas: (1) We used flux swings for each alloy that have been reproduced on multiple samples, despite having some higher flux swing results from single samples. (2) We used conservative rise and fall times for core pulsers. (For example, only 200 ns out of a 410 ns pulse is usable for beam acceleration with a 100 ns rise time and a 300 ns fall time. This is shown experimentally in Fig. 1(b) where 3.3 μs out of a 5.5 μs experimental pulse was useably flat, assuming that additional tweaking could flatten the pulse to within the required $\sim 1\%$.) (3) We kept the accelerator radius at a constant value of 1 m, rather than tapering down to 0.5 m at higher energy [2]. The latter two items led to a factor of near 3 more mass of induction cores for this work than quoted by Ref. [2]. Because core losses are proportional to the core mass, or volume, the efficiency measurements in this paper are lower than might be achievable.

Both our conservative and our challenging assumptions identify areas where further research and development could increase the performance/cost ratio of induction accelerators.

2. Experimental setup

Experimental measurements of core performance are accomplished with two pulsers. One pulser uses a thyatron to switch a 1 μF d capacitor bank through a 1–40 turn primary winding. The experimental procedure with this pulser has been described previously [3] and extensive results published [4]. A series of such measurements give the core loss (J/m^3) as a function of the magnetization rate (dB/dt) for various flux swings. We always multiply the geometric core volume by the

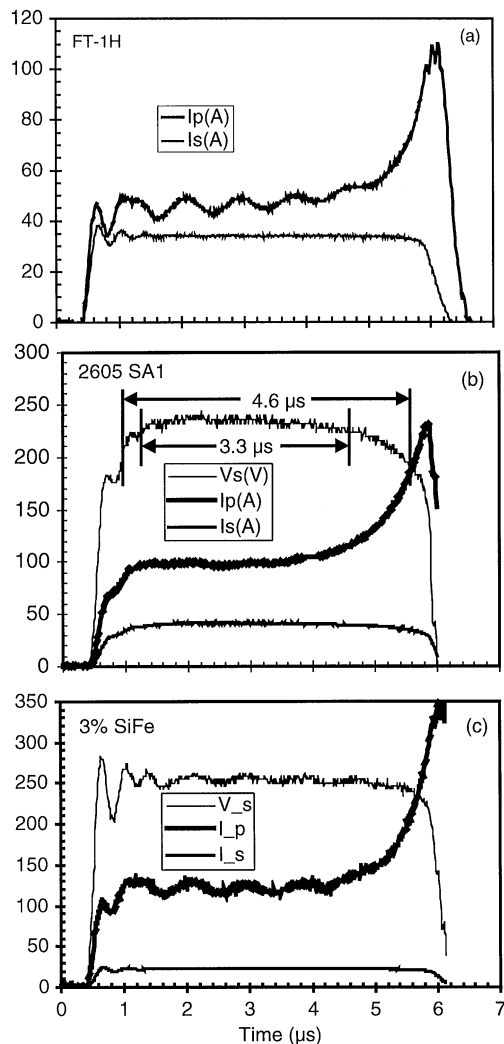


Fig. 1. (a) The primary I_p , upper, and secondary current I_s , lower, both in amperes, with an 11.4Ω secondary resistor for FINEMET FT-1 H, core 982-3, shot 4556. (b) Similar displays of current plus the secondary voltage V_s , upper in Volts, with a 5.7Ω secondary resistor for METGLAS 2605 SA1. Optimistic and conservative usable portions of the pulse are indicated for core-02, shot 4534; (b) Similar with an 11.4Ω secondary resistor for 3% silicon steel, core-2, shot 4569.

packing fraction of metal, so the core loss is given relative to the volume of an equivalent solid metal core. The voltage that would accelerate a beam is measured across an open single-turn secondary winding.

The second pulser uses an array of 2000 FETs to switch a 14.5 μF d capacitor. The FET switch

remains closed only as long as it is gated on, so that the capacitor bank does not dump completely each pulse (unlike the thyatron pulser); in most cases the voltage decreases by only a percent or so. This enables the pulser to operate in a repetitive mode, 5 Hz for the measurements presented here, which approximates the rate expected in an Heavy-Ion Fusion (HIF) power plant, such as the HYLIFE-II [5]. We approximate the energy gain of the beam with a resistive load across the secondary. The next section describes how we determine the appropriate resistance.

We made no effort to eliminate the ringing at certain pulse durations, as seen in Fig. 1a and c, in the belief that such ringing has little effect on the accuracy of measuring core losses and flux swings, our main needs. When pulsers are operated at a fixed duration with a particular design of core, they can be optimized further; so we select portions of the pulse as usable for which, in our judgment, the pulse could be flattened sufficiently ($\sim 1\%$ variation) with reasonable effort. For example, pulsers for DARHT maintain a flattop within a $\pm 0.5\%$ [6].

3. Scaling driver to test cores

To measure efficiencies with the FET pulser, that are near those expected in a power plant, we need to maintain the same ratio of beam energy gain to core loss. The core loss scales linearly with the core volume, so we scale the beam current similarly. To accomplish this, we designed a power-plant driver subject to three constraints: (1) Target designs determine the target gain G , the ion energy (GeV), and the total beam energy (MJ) required. (2) Voltage holding determines how closely cores can be packed into arrays. (3) Quadrupole magnet beam transport limits, for charge per unit length, determine the beam duration (from which we obtain the core pulse duration) versus beam energy and the subtotal mass of cores in each section of the accelerator, below a few hundred MeV. Above a few hundred MeV, the beam duration is limited to be 200 ns, which is a few times the sum of expected induction pulse rise and fall times. From (1), the total gain in energy

required for a Kr^+ beam is 1.3 GeV, which with (2) and (3) determines the total mass of cores in the accelerator. From previous measurements of core losses as a function of dB/dt , we can then compute the acceleration efficiency in the driver. The same efficiency can be measured with test cores by scaling the ratio of beam energy gain to core losses. The test cores were operated at 5 Hz with a resistor in the secondary winding to simulate the beam energy gain. The details are discussed below.

The present target designs use two energies of ion beams. For the close-coupled target, a “foot” beam of 30 ns duration, 0.85 GeV Kr^+ , delivers 0.5 MJ. The “main” pulse of 8 ns follows with 1.3 GeV Kr^+ to deliver 2.8 MJ, where we have scaled the ion energy from the 2.2 and 3.5 GeV, which was specified for lead ions [7], by the ratio of the ion masses. This maintains an approximately constant ion range in the target. The total charges in the foot and main beams, to give the beam energy for the listed ion energy, are 0.588 and 2.154 mC, yielding a total charge q of 2.742 mC. The total beam current at the injector, if the beam duration is $\sim 20 \mu\text{s}$ [2], is then

$$I = q/t_b = 0.002742/20 \times 10^{-6} = 137 \text{ A} \quad (1)$$

The cross-sectional area of individual cores in a power plant driver accelerator will be chosen to be compatible with the pulsers that are developed for the driver. Likewise, we choose the cross-sectional area of our test cores to be compatible with the two existing pulsers, each of which can switch $\sim 10 \text{ kV}$. Faraday’s Law, for the core flux swing, ΔB , and the geometrical core cross-sectional area, A , corrected by the packing fraction ε_{PF} to represent the equivalent area of solid metal, is expressed

$$V(V) = [\Delta B(T)/\Delta t(s)] \varepsilon_{\text{PF}} A(\text{m}^2). \quad (2)$$

We compute the number of concentric cores arrayed radially to produce an acceleration field of 2 MV/m, greater than conventionally used. We include sufficient radial gaps between concentric cores and axial gaps to the next array to provide a plausible possibility of holding the voltage without breakdown and supporting the weight of the core.

Our present assumptions are that we can hold 60 kV/cm across a gap with gas insulation, and that 0.25 cm of structure is required for each ton of core. Experiments are needed to refine these assumptions.

We fix the power plant accelerator radius at $r = 1$ m. The inner radii of the core arrays begin here. A more sophisticated systems code starts at $r = 1$ m, then decreases the radius to 0.5 m as increasing beam velocity allows magnetic quadrupole transport at smaller beamlet radii. It assumes Rb^+ ions, which have essentially the same mass and performance as Kr^+ [2].

The concentric arrays of cores are repeated axially until the required ion energy is reached. Since the core losses increase with core volume, the outer cores in a concentric array of similar cross-section cores will have higher losses. We compute the total loss in an array, and compare that with the beam current and energy gain for scaling to a test core.

The line charge λ of ions, in a single channel, with charge e (electron charges), mass M_i (amu), and energy E (eV) that can be transported by magnetic quadrupoles with an occupancy factor η and magnetic field B (T) at the beam radius a (m) is given by Ref. [8]

$$\lambda(\mu\text{C}/\text{m}) = 10\eta Ba \sqrt{\frac{E}{1.0 \times 10^6}} \sqrt{\frac{133e}{M_i}}. \quad (3)$$

We take advantage of the increase in λ with E , to decrease the axial length and duration of the beam to maximize the core performance as discussed below.

The beam duration begins at $\sim 20 \mu\text{s}$ at the injector, and is decreased as fast as possible, limited by magnetic quadrupole transport, until a 200 ns duration is reached, and main-

tained through the rest of the accelerator. The beam charge remains constant so the current increases as $(\text{duration})^{-1}$. Since the core cross-sectional area and flux swing yield the core performance in “volt-seconds”, we obtain the maximum acceleration in volts with minimum core area and mass by minimizing the beam duration, consistent with Faraday’s Law, Eq. (2).

The core pulse duration Δt is longer than the beam duration, to include rise and fall times of the core and the beam. The core pulser rise time is assumed to have 3 values: $1 \mu\text{s}$ for $5\text{--}20 \mu\text{s}$ beam durations, $0.3 \mu\text{s}$ for $1\text{--}5 \mu\text{s}$ beam durations, and $0.1 \mu\text{s}$ for beam durations below $1 \mu\text{s}$. Core fall times that are three times the rise time are assumed. This is characteristic of PFN (Pulse-Forming-Network) performance with moderately good, but not the lowest inductance capacitors. The beam rise and fall time is 700 ns at the injector, decreasing linearly with the beam duration to 7 ns. We estimate the equivalent square pulse duration in order to evaluate the core cross-section required to induce a given voltage along the beam: First, we approximate the core rise and fall as triangular and take half the sum of these durations. Second, we add it to the sums of the beam rise, fall, and duration to get the effective core pulse duration. The beam rise and fall times must fall completely within the flat portion of the core pulse, so we make no duration correction for the shape of the rise and fall.

For a given core alloy, cross-sectional area, and $(\Delta B/\Delta t)$ we obtain the same voltage in a test core or in a driver core. The core losses will vary proportionally to the volume. For our test cores, the resistances listed in Table 1 yield a similar efficiency with the FET pulser as are expected with a driver scale induction accelerator with a Kr^+ beam.

Table 1

Performance of three alloys, and resistors needed to simulate driver performance with our test core

Alloy	ID (cm)	OD (cm)	Width (cm)	ΔB (T)	Reset (A-t)	Loss (J/m ³) (0.4 μs)	Acceleration efficiency (0.4 μs)	R (Ω)
Finemet FT1H	6.0	15.6	2.54	2.2	3	770	0.67	11.4
METGLAS 2605 SA1	13.1	18.0	2.51	2.2	7.5	1810	0.47	5.68
3% SiFe	8.2	11.4	3.81	2.8	40	3080	0.37	11.4

4. Measurements

We selected cores of three magnetic alloys for evaluation, with properties that are summarized in Table 1. Each type had an insulating coating, to prevent the flow of interlaminar eddy currents, and was magnetically annealed after winding to increase the flux swing and minimize core losses [3]. Honeywell (formerly AlliedSignal) METGLAS 2605 SA1 was developed for high-efficiency 60 Hz transformers, and is at present the least costly material. Compared with the pulsed power alloy 2605 SC, it has been demonstrated to give similar flux swings and slightly greater losses, and it is easier to work with. The core used here had a low ratio of remanent field B_r to saturation field B_s , $B_r/B_s = 0.5$, which led to lower flux swings than observed previously with 2605 SA1 [4]. The core tested earlier was no longer available. Hitachi FINEMET FT-1 H was selected for its low loss, and moderate flux swing. The core used here, LBNL-982-3, was among those tested before [4], but yielded an enhanced flux swing of 2.2 T with the DC reset current used here. The third alloy, 3% silicon steel, is a standard material for 60 Hz transformers. Here, we use a thinner version, which we label P-1, with 25 μm thick laminations which is comparable to the thickness of METGLAS and FINEMET. Silicon steel has $3.5 \times$ higher loss than 2605SA1, and requires a much higher reset current. It may still be attractive near the injector, because its larger flux swing allows a $7 \times 10^5 \text{ kg}$ reduction in mass at the expense of a 340 kW increase in pulser power over the first 6 MeV of acceleration in a 1000 MW_e power plant driver. The core inner and outer diameters and widths are listed in Table 1.

The DC reset current, listed in Table 1, was chosen as a compromise to maximize the flux swing with a minimal increase in drive current. Some of the enhanced flux swing performance of FT-1 H may be due to the ease of exceeding its reset current threshold.

The differing beam acceleration efficiency of core materials is shown in Fig. 1(a)–(c), by the ratio of the measured current (A turns) in the single turn secondary I_s to that in the multi-turn primary I_p . The difference, due to core losses, is

much larger for 2605 SA1, Fig. 1(b), and especially 3% silicon steel, Fig. 1(c), than for FT-1 H, Fig. 1(a). The primary current is the sum of the current needed to drive the secondary current plus the current needed to drive the core losses (eddy current losses in each lamination). Fig. 1(b) and (c) also shows the secondary voltage V_s , which is equal to the secondary current times the secondary resistance of 5.7Ω in Fig. 1(b) and 11.4Ω in Fig. 1(c). In Fig. 1(a), the secondary resistance is 11.4Ω , so that the secondary voltage of nearly 400 V would be off scale. The inferred efficiencies seem relatively low, but this is due to the long pulse durations in Fig. 1. The efficiencies are in agreement with those in Fig. 2, for magnetization rates of 0.3–0.4 T/ μs .

The beam acceleration efficiency, relative to the power into the cores, is plotted directly in Fig. 2 for the three alloys: FINEMET FT-1 H (squares), METGLAS 2605 SA1 (triangles), and 3% silicon steel (Circles). The acceleration efficiency ϵ_a is defined by

$$\epsilon_a = \left(\frac{\int_0^{\Delta t} (V_s^2/R) dt}{\int_0^{\Delta t} (V_s^2/R) dt + \int_0^{\Delta t} V_s I_p dt} \right) \quad (4)$$

Both the energy to the secondary resistor and the losses are integrated from the beginning of the pulse to the end of the usefully flat portion of

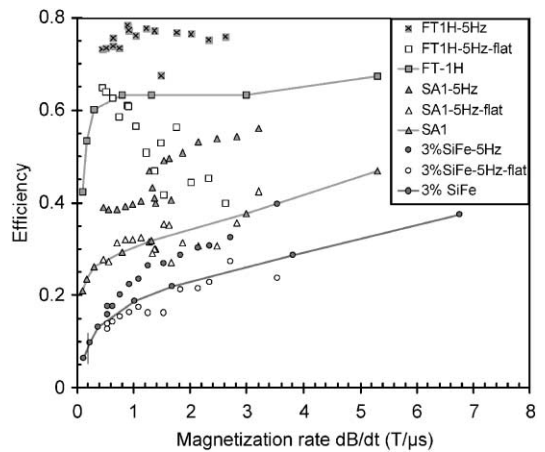


Fig. 2. The acceleration efficiency for three alloys: FINEMET FT-1 H (squares), METGLAS 2605 SA1 (triangles), and 3% silicon steel (circles). Optimistic (filled) and conservative (open) data points are shown.

the pulse Δt . (We did not subtract the secondary-resistor energy preceding the $4.6\mu\text{s}$ portion of the pulse in Fig. 1b. This would have reduced the efficiency from 0.40 to 0.39, for example.)

The results shown by lines through data points are fits to data from the thyatron pulser. The results shown by data points, without a line, are from repetitive pulsing of the FET pulser. For the filled data points, we select the maximum portion of each voltage waveform that could possibly be made usable by more optimal design of each pulser, as shown by the $4.6\mu\text{s}$ portion in Fig. 1(b). The end of the maximum duration useful pulse is defined as the time at which the voltage sags faster than linearly; then it can no longer be approximated by a square pulse plus a triangular pulse to counteract the sag. This is also how we define the maximum usable flux swing, except that we then applied the same flux swing to every shot, whereas the maximum pulse duration was determined for each shot. For the open data points, we select a 5% wide band, as shown by the $3.3\mu\text{s}$ portion of Fig. 1(b). We expect that the 5% width could be reduced to 1% (acceptable limit for heavy-ion fusion) by optimizing each pulser for the type of core and the pulse duration. With the open data points, a smaller fraction of the induction pulse is used to accelerate beam, so the accelerator efficiency is lower, near or below the line in Fig. 2. The differences between the three data sets for each core result from differing criteria for the useful fraction of the pulse, and the scatter in each data set is primarily due to uncertainties in measuring the duration of the sufficiently flat portion of the pulse.

The efficiency increases slowly with dB/dt , despite the core losses increasing as fast as linearly with dB/dt , because the energy to the resistor or the beam increases even more rapidly. From Eq. (2), $V \propto dB/dt$ and the power to the secondary resistor is $P = V^2/R \propto (dB/dt)^2$. The dynamic impedance of the beam approximates a constant current source, which is very different from a resistive impedance. Yet, surprisingly, the scaling with beam is nearly identical, because $P = VI$ and from Eq. (1), $I \propto 1/t \propto dB/dt$ for constant dB , so again, $P \propto (dB/dt)^2$. The resistive loads, therefore, provide the same scaling of efficiency with

magnetization rate as would a beam; except that the power to a resistive load is not the same as to a beam during the rise and fall of the pulse, which will be timed to occur when the beam current is zero.

Core heating is estimated to be a very slow process, heating a core at less than $1^\circ\text{C}/\text{min}$, even for the highest loss 3% silicon steel core at $dB/dt = 7\text{ T}/\mu\text{s}$. For such low rates of heating, gas cooling should be sufficient.

With the caveats listed below, we also estimated the net efficiency defined as the ratio of the usable average power in the secondary resistor to the power supply output power, that charges the capacitor. This includes losses in the FET pulser switch and charging. We made one correction—we subtracted the portion of the power-supply current necessary to keep the bank charged at a zero pulse rate, which is equivalent to a $3\text{ M}\Omega$ resistor across the capacitor. Even though the net efficiency is the value we would most like to know because it is most closely related to overall power plant efficiency, it is less fundamental because it depends on the pulser and charging system design as well as on the core alloy and mechanical layout. With the FET pulser and $1\mu\text{s}$ pulses, the net efficiencies for the three alloys, FT-1H, 2605 SA1, and 3% silicon steel, were 0.37, 0.30 and 0.20, respectively. These compare with the acceleration efficiencies for $1\mu\text{s}$ pulses, based only on core losses, of 0.75, 0.52, and 0.32, respectively. The difference between the net and acceleration efficiency is due to losses in the pulsers. Pulsers designed with efficiency in mind may therefore provide higher net efficiencies.

We can gauge the acceptability of the above efficiencies using some rules-of-thumb. First we use an estimate of 5 MW_e for all other losses in the accelerator such as refrigeration power for superconducting magnets and vacuum pumping [9]. Then we use the inertial fusion energy rule of thumb $\eta G \geq 10$ [10], where η is the driver efficiency and G is the target gain. (Satisfying the criterion $\eta G \geq 10$ assures that the recirculating power in a power plant is less than 20–25%.) With current distributed-radiator, heavy-ion target designs $65 \leq G \leq 130$ [7]. With the above net efficiencies plus another 5 MW_e loss in the driver, we obtain $12 \leq \eta G \leq 43$, exceeding the minimum requirement.

Even 3% silicon steel, with its $\sim 20\%$ net efficiency, might be marginally acceptable to use for an entire driver. Moreover, 3% silicon steel would have little effect on the overall efficiency if its use were restricted to the injector region, where its higher flux swing would reduce the mass of induction cores. We conclude that the acceleration and net efficiencies are sufficient to satisfy rules of thumb by a significant margin.

5. Summary

We obtained encouraging measurements of efficiency with a 5 Hz pulser, using resistors to simulate the beam energy gain in an accelerator. The resistors were scaled from our present concept of the optimum core array geometry; and, as we showed, provide the same scaling of efficiency versus dB/dt as would a beam, except during the rise and fall of the core pulse when the beam current would be zero. Our baseline amorphous alloys provide $\eta G \geq 18$, well in excess of 10. Amorphous or nanocrystalline alloys, together with the high-gain target designs and high-efficiency pulsers could provide ηG of 35–43, including another 5 MW of driver power losses. The results in this paper should be taken as indicative of the range of performance to be expected. Precise core and pulser performance is only determined when the full-scale components for a given facility are tested together. We expect most of the changes in flux swing and efficiency with full scale units to be in a favorable direction: improved quality control of core manufacturing may routinely yield the higher flux swings that are occasionally seen today; larger-radius small-build-up cores will be under less mechanical stress

which could increase flux swing and reduce losses; total core mass is likely to be reduced from the assumptions made here; and pulsers will be designed for efficiency and short rise and fall times as well as accuracy and long life.

Acknowledgements

We thank Roger Bangerter for his support and critiques of this work. This work was performed under the auspices of the US Department of Energy by University of California Lawrence Livermore National Laboratory under contract No. W-7405-Eng-48, and Lawrence Berkeley National Laboratory under contract No. DE-AC03-76F00098.

References

- [1] R.O. Bangerter, *Il Nuovo Cimento* 106 (1993) 1445.
- [2] W.R. Meier, J.J. Barnard, R.O. Bangerter, *Nucl. Instr. and Meth. A* 464 (2001) 433, this proceedings.
- [3] A.W. Molvik, A. Faltens, L. Reginato, M. Błaskiewicz, C. Smith, R. Wood, *Nucl. Instr. and Meth. A* 415 (1998) 315.
- [4] A.W. Molvik, W.R. Meier, A. Faltens, L. Reginato, C. Smith, Induction core performance, Proceedings of Linac98 Conference, 1998. Available at <http://www.aps.anl.gov/conferences/LINAC98/>
- [5] R.W. Moir et al., *Fusion Technol.* 25 (1994) 5.
- [6] W. Waldron, L. Reginato, private communication, 2000.
- [7] D.A. Callahan-Miller, M. Tabak, *Nucl. Fusion* 39 (1999) 1547.
- [8] E.P. Lee, R.J. Briggs, The solenoidal transport option: IFE Drivers, Near Term Research Facilities, and Beam Dynamics, Report LBNL-40774, 1997.
- [9] W. Meier, private communication, 1998.
- [10] J. Lindl, *Phys. Plasmas* 2 (1995) 3933.